

# Shell-like configuration in $O^+$ ion velocity distribution at high altitudes in the dayside magnetosphere observed by Cluster/CIS

S. Joko<sup>1</sup>, H. Nilsson<sup>1</sup>, R. Lundin<sup>1</sup>, B. Popielawska<sup>2</sup>, H. Rème<sup>3</sup>, M. B. Bavassano-Cattaneo<sup>4</sup>, G. Paschmann<sup>5</sup>, A. Korth<sup>6</sup>, L. M. Kistler<sup>7</sup>, and G. K. Parks<sup>8</sup>

<sup>1</sup>Swedish Institute of Space Physics (IRF), P.O. Box 812 SE-98128 Kiruna, Sweden

<sup>2</sup>Space Research Center (P.A.S.), Warsaw, Poland

<sup>3</sup>Centre d'Etude Spatiale des Rayonnements, Toulouse, France

<sup>4</sup>Instituto di Fisica dello Spazio Interplanetario, Roma, Italy

<sup>5</sup>Max-Planck-Institut für Extraterrestrische Physik, Garching, Germany

<sup>6</sup>Max-Planck-Institut für Aeronomie, Katlenburg-Lindau, Germany

<sup>7</sup>University of New Hampshire, Durham, USA

<sup>8</sup>Space Science Laboratory, UC Berkeley, USA

Received: 8 August 2003 – Revised: 21 May 2004 – Accepted: 28 May 2004 – Published: 14 July 2004

Part of Special Issue “Spatio-temporal analysis and multipoint measurements in space”

**Abstract.** We report shell-like configurations seen in  $O^+$  ion velocity distributions. One case was observed above  $8 R_E$  in radial distance in the dayside magnetosphere, presumably in the mantle region, during the observation period of 09:30–10:00 UT on 12 April 2001 by the CIS instrument on board the Cluster satellite. This shell-like configuration was different from so-called “conics” or “beams”: the lower energy (cold) population and the higher energy partial shell part were seen together, but there was no obvious signature of heating process. With respect to  $H^+$  ion velocity distributions observed simultaneously, transverse heating (so-called in “pan-cake” shape) or field-aligned energisation configurations were seen as the result of heating/energisation processes and the upward-going part of the distribution also formed a half spherical thick shell configuration. Concerning  $O^+$  ion heating in the case of 12 April 2001, it was obviously observed when the spacecraft passed through the mantle region close to the poleward cusp. As the spacecraft moved toward the dayside cusp shell-like (or dome shape) velocity distributions appeared apparently and continued to be observed until the spacecraft reached the magnetopause according to two other different cases (13 February 2001 and 14 April 2001). Two other cases were observed in the Southern Hemisphere and the spacecraft was supposed to pass through the dayside cusp toward the mantle region at higher altitudes ( $9\text{--}11 R_E$ ).  $O^+$  ion velocity distributions in these cases show pre-/post-structured shell-like configurations, depending on the observation sites (mantle or dayside cusp).

**Key words.** Magnetospheric physics (magnetopause, cusp, and boundary layers; magnetospheric configuration and dynamics; general or miscellaneous)

## 1 Introduction

Ion outflows in the cusp region have been greatly studied previously and ionospheric ion outflows in this region have been reported as persistent phenomena (Yau and André (1997)). It is believed that ion outflows are accompanied by transverse ion heating and one of the probable explanations for transverse ion heating is a wave-particle interaction. Numerous satellite crossings of the dayside cusp region have yielded observations that suggest one or more wave modes as the agents of plasma heating. Freja observations at the altitudes below 1700 km (Nordqvist et al. (1998)) and FAST satellite observations at the altitudes below 4000 km (Lund et al. (2000)) showed that most transverse ion heating events were associated with an enhancement of broad-band, extremely low frequency (BBELF) turbulence. In those cases, ions obtained energies through cyclotron resonance around the ion frequencies.

Another possible wave mode causing transverse ion heating is an electrostatic wave around the lower hybrid (LH) frequency, e.g. Bouhram et al. (2002). Roth and Hudson (1985) demonstrated that ring distributions of magnetosheath ion injections, observed by both S3-3 and Dynamics Explorer-1 (DE-1) at  $\sim 1\text{--}4 R_E$ , can generate LH waves by means of kinetic simulations.

On the one hand, energetic (>40 keV) ions have been observed in the dayside high-altitude (6–9.2  $R_E$ ) cusp regions by the Polar satellite (Chen et al. (1997); Chen and Fritz (2001); Fritz et al. (2003) for the latest and references therein). These energetic ions seemed to be associated with large diamagnetic cavities, perhaps caused by strong magnetic field turbulences, and the cusp diamagnetic cavities were almost always observed. On the other hand, simultaneously observed lower energetic (>20 keV) ion fluxes were reported to be observed in the dayside high-latitude magnetosheath, rather than in the cusp cavities, under the condition of high solar wind pressure. In fact, these lower energetic ion fluxes were reported from another point of view. The magnetosheath ions of  $\sim 2$  keV as a maximum energy under the low solar wind dynamic pressure observed by the Cluster satellite showed highly isotropized velocity distributions (Lavraud et al., 2002). In contrast, this paper presented outflowing ions (both H<sup>+</sup> and O<sup>+</sup>) having energies ranging  $\sim 2$ –20 keV observed from the mantle region, dayside cusp, and to the magnetopause at around 8  $R_E$  in radial distance that showed another feature; both H<sup>+</sup> and O<sup>+</sup> ions had non-isotropized velocity distributions. For both outflowing H<sup>+</sup> and O<sup>+</sup> populations, Peterson et al. (1993a, 1993b) interpreted the energisation and transport of ions, on basis of the observations by the Akebono and DE-1 satellites at altitudes  $\sim 5000$  and 22 000 km, in terms of a standing Alfvén wave using coincident observations of magnetic field perturbation.

This paper will discuss shell-like configurations seen in O<sup>+</sup> ion velocity distributions, a kind of non-Maxwellian or non-isotropic particle distribution, and this type of velocity distribution has been reported firstly from the cometary plasma studies e.g. Mukai et al. (1986); Neugebauer et al. (1987). Gary et al. (1988) have investigated wave-particle interactions of two pick-up ion species, i.e. H<sup>+</sup> and O<sup>+</sup> ions by means of one-dimensional electromagnetic hybrid simulations of homogeneous plasma. Gary et al. (1988) found that 1) pitch-angle scattering promotes the formation of thin shell-like velocity distributions of pick-up cometary H<sup>+</sup> ions first in time-scale, and 2) as the O<sup>+</sup> ions are scattered into a shell-like distribution the pick-up H<sup>+</sup> ions were found to be subject to stochastic acceleration. Their investigation with computer simulations was based on the growth of plasma instabilities that are considered to enhance large-amplitude low-frequency fluctuations in the magnetic field, and then the enhanced fluctuations in the magnetic field  $(\Delta B/B)^2$  act to isotropize ions by pitch angle scattering. Concerning another case observed near at the Earth, Fuselier et al. (1988) (1988) reported solar wind He<sup>++</sup> and O<sup>6+</sup> shell-like distributions in the magnetosheath. Both He<sup>++</sup> and O<sup>6+</sup> distributions are centred on the downstream H<sup>+</sup> bulk velocity and Fuselier et al. (1988) suggested the formation of shell-like distributions might occur through a coherent wave-particle interaction and/or by scattering in the existing magnetic turbulence in the sheath. The shell-like O<sup>+</sup> velocity distributions presented in this paper were observed in the mantle region and the dayside cusp and the shell-like (or dome shape) velocity distribution observed in the cusp should be discussed in

terms of heating process. Roth and Hudson (1985), as cited shortly above, reported that O<sup>+</sup> ions originating in the ionosphere are heated significantly by He<sup>++</sup> ions in the inflowing solar wind that downflow into the cusp. In that case, downflowing He<sup>++</sup> ions have a ring-shaped velocity distribution and low hybrid (LH) waves are excited mainly perpendicular to the geomagnetic field by the ring distribution. These LH waves play an important role in heating/energising O<sup>+</sup> ion conics. With respect to generating “ring” (or “toroidal”) distributions, Moore et al. (1986) suggested a coherent acceleration and Brown et al. (1991) did velocity filter effects.

## 2 Data

### 2.1 Observation conditions

One observation was done by the Cluster satellite on 12 April 2001, from 08:00–11:00 UT. The Cluster spacecraft-4 (hereafter S/C-4) passed through the mantle region close to the poleward cusp (magnetic latitude, MLAT hereafter, was 75.7°, magnetic local time, MLT, was 12.1 h, and radial distance was 7.6  $R_E$  at 09:00 UT), moved toward the high-altitude dayside cusp/the magnetopause in the pre-noon sector after 10:00 UT (MLAT=70.1°, MLT=11.0, and 8.7  $R_E$ ). During this period, the interplanetary magnetic field (IMF) was a northward ( $B_z > 0$ ),  $-B_y$ -dominant ( $B_y \approx -20$  nT). Actually there was a strong coronal mass ejection (CME) event and it impacted the magnetosphere on the previous day. The geomagnetic activity was high according to the  $K_p$  index ( $K_p=5$ ).

Other two cases were observed on 1) 13 February 2001, 19:00–22:00 UT, and 2) 14 April 2001, 06:30–09:30 UT, respectively. The summary of those observations are: 1) the S/C-1 passed through from {MLAT= $-45.2^\circ$ , MLT=13.1, and 10.7  $R_E$  at 19:00 UT} to {MLAT= $-72.1^\circ$ , MLT=14.8, and 7.5  $R_E$  at 22:00 UT}. The IMF condition was southward, the  $B_y$  component was fluctuating but not with large amplitude, and  $B_x$  was constantly minus (0 to  $-4$  nT).  $K_p$  indices were 4 to 5-. (2) the S/C-3 passed through from {MLAT= $-56.6^\circ$ , MLT=8.4, and 11.6  $R_E$  at 06:00 UT} to {MLAT= $-67.0^\circ$ , MLT=7.6, and 8.7  $R_E$  at 09:00 UT}. The IMF condition was  $-B_y$  dominant ( $\sim 10$  nT) and  $B_z$  fluctuated between  $-3$  and 5 nT.  $K_p$  index was 3+.

Figure 1 shows time-energy spectrograms of four ion species (H<sup>+</sup>, He<sup>++</sup>, He<sup>+</sup> and O<sup>+</sup>) and geomagnetic field components for three different cases (from the top, 12 April 2001, 13 February 2001, and 14 April 2001, respectively). According to the geomagnetic field data, it is presumed that the spacecraft was in the high-altitude dayside cusp (1) from 10:00 UT intermittently on 12 April 2001, 2) through the magnetopause to 20:08 UT, and 3) 07:22–07:45 UT on 14 April 2001. In this report, O<sup>+</sup> ion velocity distributions were selected from both “not in the cusp” (probably in the mantle region) and “in the dayside cusp”, except for the case of 12 April 2001.

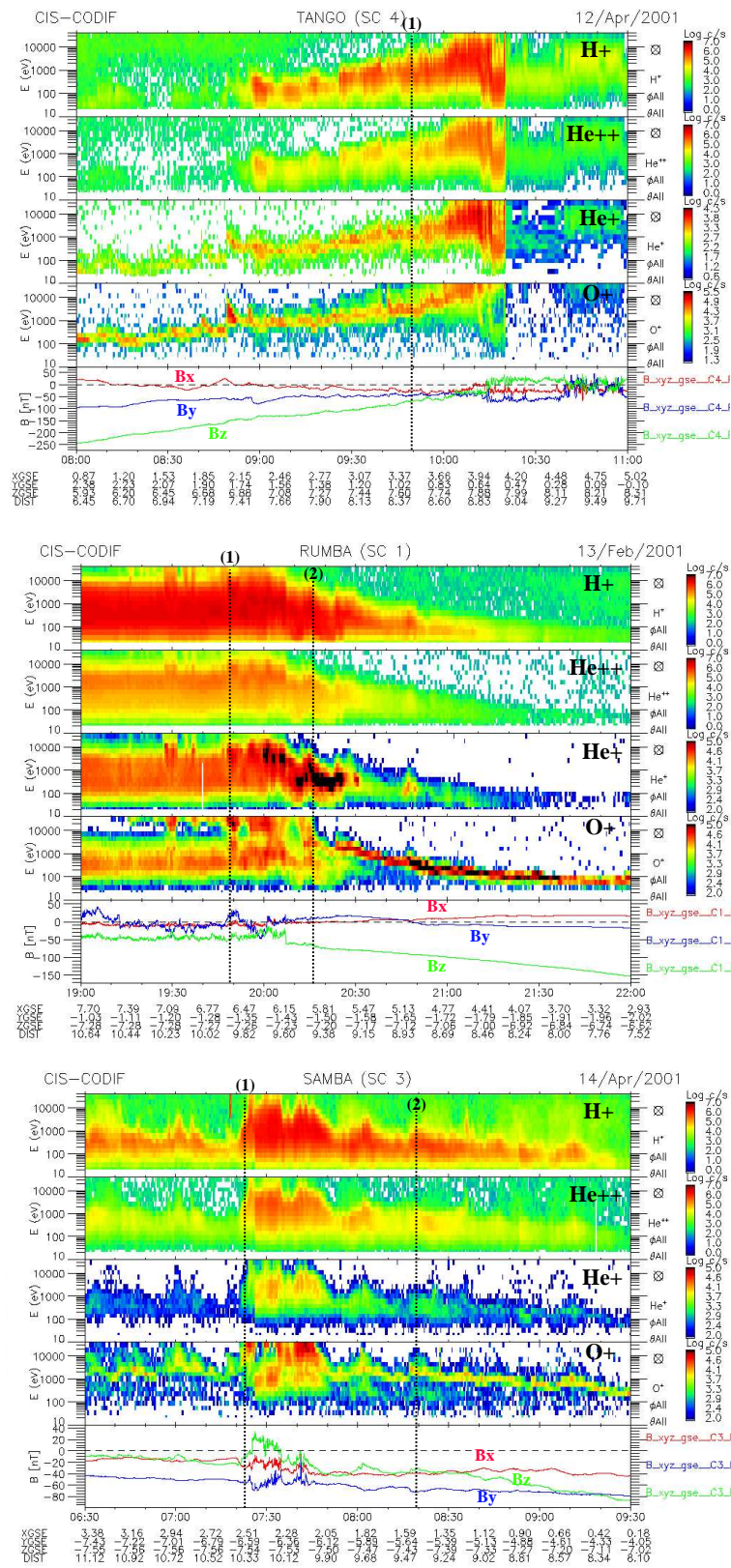


**Fig. 1.** Time-energy spectrograms of four ion species (H<sup>+</sup>, He<sup>++</sup>, He<sup>+</sup> and O<sup>+</sup>) and geomagnetic field components. From the top panel 12 April 2001, 13 February 2001, and 14 April 2001, respectively.

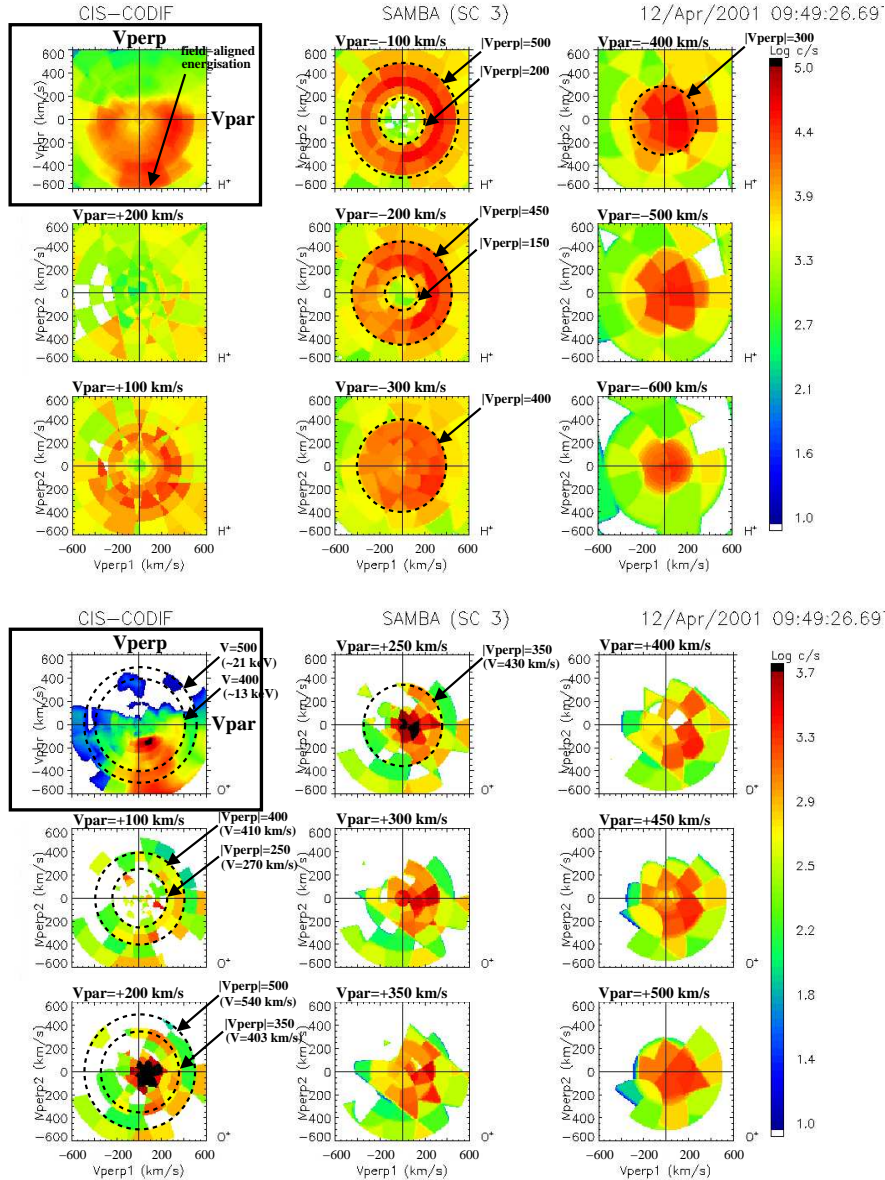


**Fig. 2.** H<sup>+</sup>(upper)/O<sup>+</sup>(lower) ion velocity distributions in counts per second (c/s) observed by the Cluster S/C-3. The  $-V_{\text{par}}$  direction corresponds to upward direction along the geomagnetic field in this case. The upper left panel in each set of velocity distributions shows a  $V_{\text{par}}-V_{\text{perp}}$  cross section and the other eight panels are cross sections in the  $V_{\text{perp}}$  plane at different  $V_{\text{par}}$  velocities.

### 2.2 Velocity distributions in the mantle region

Figure 2 shows H<sup>+</sup>/O<sup>+</sup> ion velocity distributions observed by the CIS/CODIF (Cluster Ion Spectrometry experiment/time-of-flight ion COmposition and DIstribution Function analyser) instruments on board the Cluster S/C-3. Figure 3 is comparable to Fig. 2 and the velocity distributions in Fig. 3 were observed by the Cluster S/C-4. In the time-energy spectrograms (top panel in Fig. 1), the observation time was marked by a vertical dashed line with number 1). There was a 5-s time interval between two spacecrafts and the interspacecraft distance was estimated to be about 807 km. The average speed of the spacecraft was 1.9 km/s and was a low

value compared to typical plasma velocity and convection drift ( $\sim 20$  km/s), thus the effect on plasma observation could be ignored. One velocity distribution panel was composed of a 4-spin accumulation (1 spin=4 s) and is shown in logarithmic count rate (c/s). One set of velocity distributions shown in both Fig. 2 and Fig. 3 consists of nine panels: the upper left panel shows a velocity distribution as a function of parallel ( $V_{\text{par}}$ ) and perpendicular ( $V_{\text{perp}}$ ) velocity. The other eight panels show different cross sections in the perpendicular velocity plane at different  $V_{\text{par}}$  velocities.

With respect to O<sup>+</sup> ion velocity distributions observed by both spacecrafts (lower panels in both Fig. 2 and Fig. 3), the following are seen: at  $V_{\text{par}} \sim -150$  to  $-200$  km/s (equivalent

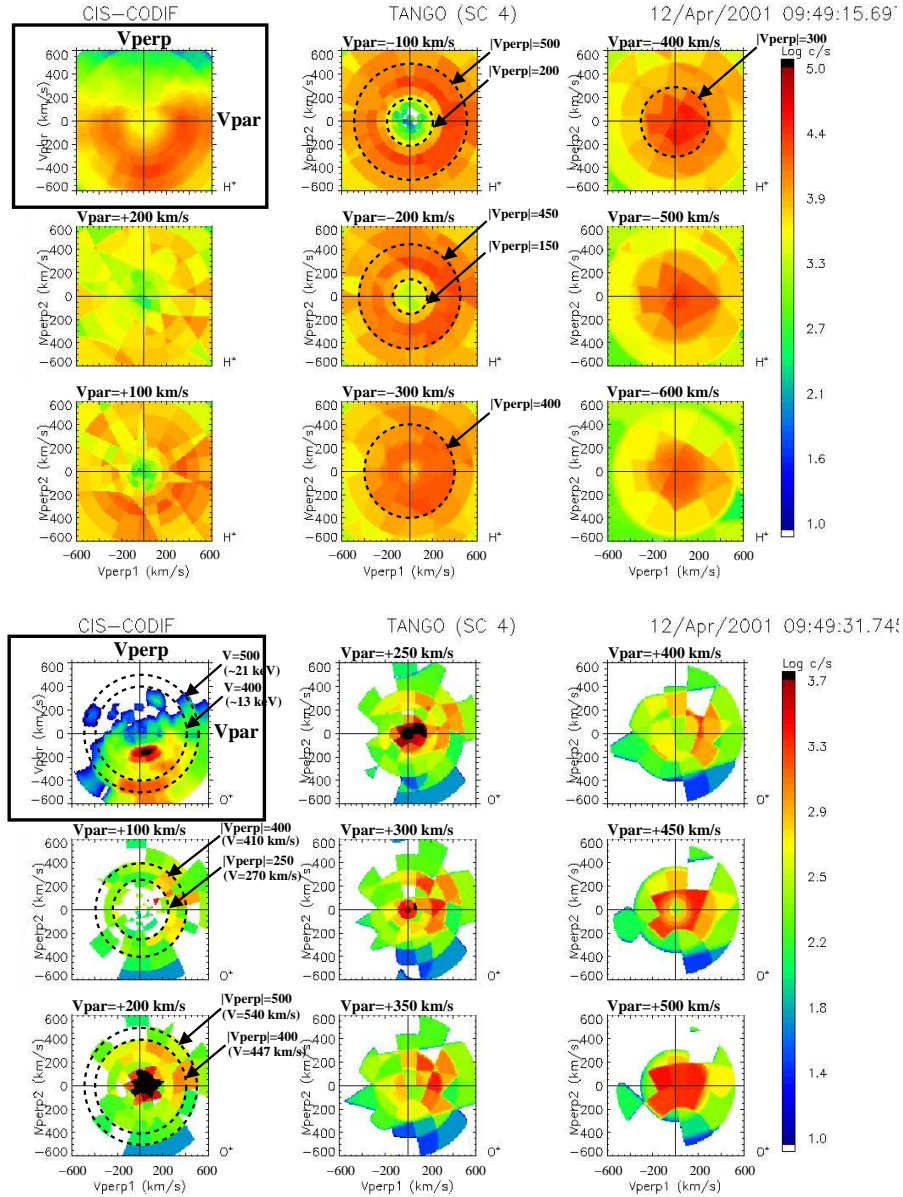


**Fig. 3.** H<sup>+</sup>(upper)/O<sup>+</sup>(lower) ion velocity distributions in counts per second (c/s) observed by the Cluster S/C-4. The construction of the panel is the same as that of Fig. 2. There was a 5-s time interval between two spacecraft and the interspacecraft distance was about 807 km. There is no available H<sup>+</sup> velocity distribution comparable to O<sup>+</sup> velocity distribution at 09:49:31 UT; therefore, the distribution at 09:49:15 UT is shown for H<sup>+</sup>.

kinetic energy ranges from 1.9~2.8 keV) in the upper left panel, an intense, relatively cold population is seen almost along the geomagnetic field. In terms of pitch angle distribution, this cold population part is distributed above 120° where polar angular resolution is 22.5° for the CIS/CODIF instrument. In the same panel, the speeds of 400 and 500 km/s are marked by dashed circles, where speed  $V$  is defined as  $V = \sqrt{V_{\text{par}}^2 + V_{\text{perp}}^2}$ , and the equivalent kinetic energies are ~13 and 21 keV, respectively. These parts have much higher energies than that of the aforementioned cold population. At  $V_{\text{par}} = -100$  km/s,  $-200$  km/s and  $-250$  km/s in each perpendicular velocity cross section, not complete but partial ring

configurations can be seen. These rings indicate a speed of either  $V \sim 400$  km/s or  $V \sim 500$  km/s, and both speeds are shown by dashed circles in the  $V_{\text{par}} - V_{\text{perp}}$  cross section in the upper left panels, as mentioned previously. The energy resolution of the CIS/CODIF instrument is  $\Delta E/E = 0.16$ , so that the velocity resolution is considered to be  $\Delta V/V = 0.08$ . Therefore, a partial spherical shell configuration was presumably observed in the O<sup>+</sup> ion velocity distribution due to the velocity resolution. Two set of O<sup>+</sup> ion velocity distributions observed by two different spacecraft, where the interspacecraft distance was estimated to be about 807 km, can support this presumption.

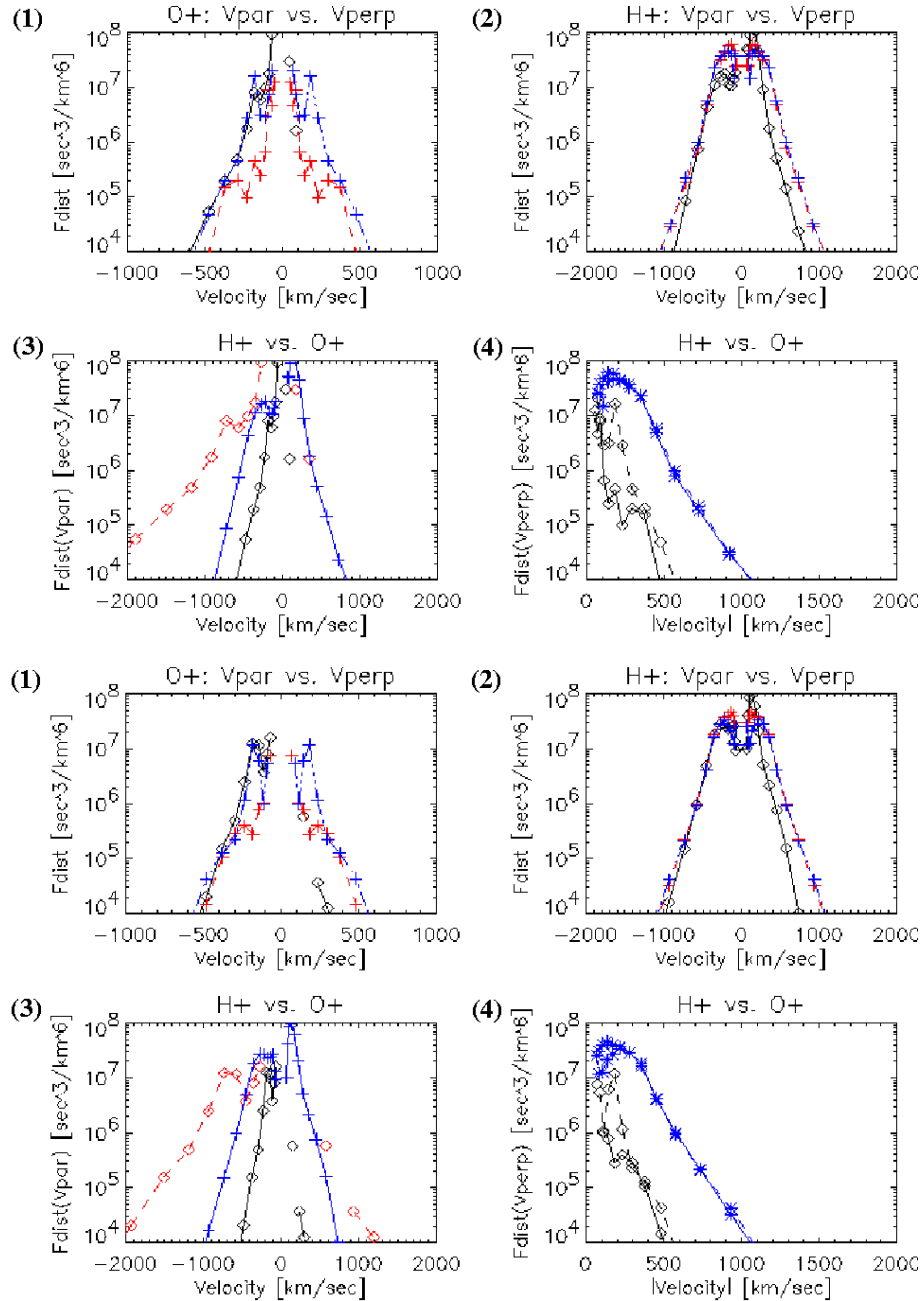


**Fig. 4.** The distribution functions ( $f(V_{\text{par}})$  and  $f(V_{\text{perp}})$ ) of  $H^+/O^+$  ions observed by the Cluster S/C-3 at 09:49:26 UT (upper panel) and by the Cluster S/C-4 at 09:49:31 UT (lower panel). These observations are done by adjoining two spacecraft. The construction of the panels is explained in the text.

On the other hand, as to the simultaneous  $H^+$  velocity distributions shown in the upper panels of Fig. 2 and Fig. 3, respectively, a shell-like configuration was also seen in addition to transverse heating or field-aligned energisation. Actually a shell configuration seen in  $H^+$  velocity distribution was thicker in the velocity range, i.e. heated, and formed almost a half spherical shell in the upward direction along the geomagnetic field. The speed ( $V$ ) of the half spherical shell configuration ranged from 220 ( $\sim 250$ ) to  $\sim 500$  km/s, and the maximum speed corresponds to the maximum speed of the

higher energy shell-like part seen in the  $O^+$  ion velocity distribution.

Figure 4 shows distribution functions ( $f(V_{\text{par}})$  and  $f(V_{\text{perp}})$ ) of both  $H^+$  and  $O^+$  observed at 09:49:26 UT by the Cluster S/C-3 and at 09:49:31 UT (for  $H^+$  09:46:15 UT) by the Cluster S/C-4. The unit of the distribution function is  $s^3/\text{km}^6$  and shown by logarithmic scale, and  $f(V_{\text{par}} < 0)$  corresponds to the upward-going population along the geomagnetic field in this case. One panel consists of 1) a comparison between  $f(V_{\text{par}})_{O^+}$  (black line with diamond mark) and

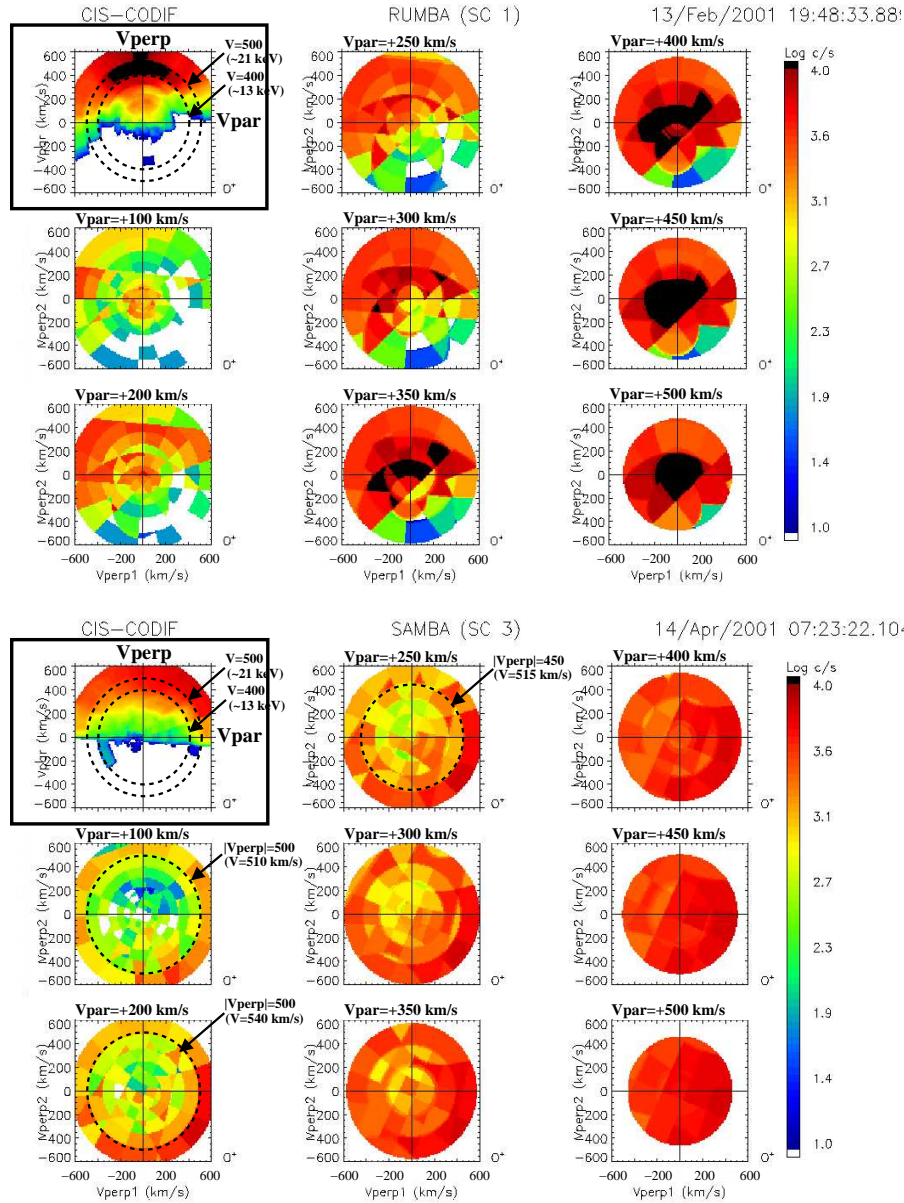


**Fig. 5.** O<sup>+</sup> ion velocity distributions in counts per second (c/s) observed by the Cluster S/C-1 on 13 February 2001 (upper) and the Cluster S/C-3 on 14 April 2001 (lower). They were presumably observed in the dayside cusp. The +V<sub>par</sub> direction corresponds to the upward direction along the geomagnetic field in these cases. The construction of the panels is the same as that of Fig. 2.

$f(V_{\text{perp}})_{\text{O}^+}$  (blue and red lines with cross mark).  $f(V_{\text{perp}})_{\text{O}^+}$  in blue corresponds to the distribution function of the pitch angles ranging from 67.5–90° in omni-azimuthal direction, and  $f(V_{\text{perp}})_{\text{O}^+}$  in red corresponds to the distribution function of the pitch angles ranging from 90–112.5° in omni-azimuthal direction; therefore, both  $f(V_{\text{perp}})_{\text{O}^+}$ s are symmetric with respect to the  $V_{\text{perp}}=0$ , 2) comparison between  $f(V_{\text{par}})_{\text{H}^+}$  (black line with diamond mark) and  $f(V_{\text{perp}})_{\text{H}^+}$  (blue and red lines with cross mark); other constructions are the same as (2), 3) comparison between  $f(V_{\text{par}})_{\text{O}^+}$  (black line with diamond mark) and  $f(V_{\text{par}})_{\text{H}^+}$  (blue line with cross mark). The function depicted by red line with the diamond mark is  $f(V_{\text{par}})_{\text{O}^+}$  but the mass is considered to be that of

H<sup>+</sup>, 4) comparison between  $f(V_{\text{perp}})_{\text{O}^+}$  (black solid/dashed lines with diamond mark) and  $f(V_{\text{perp}})_{\text{H}^+}$  (blue solid/dashed lines with cross mark). The solid line corresponds to the pitch angles ranging from 67.5–90° and the dashed one to the pitch angles ranging from 90–112.5°. According to the distribution functions,  $f(V_{\text{par}})_{\text{O}^+}$  is not a field-aligned symmetric and  $f(V_{\text{par}})_{\text{O}^+}$  and  $f(V_{\text{perp}})_{\text{O}^+}$  are also different. The O<sup>+</sup> upward-going population ( $f(V_{\text{par}}<0)$ ) seems to consist of two distributions: corresponding to a lower energy cold population and a higher energy shell-like part, as shown in O<sup>+</sup> velocity distributions. Regarding  $f(V)_{\text{H}^+}$ , both  $f(V_{\text{par}}<0)_{\text{H}^+}$  and  $f(V_{\text{perp}})_{\text{H}^+}$  seem to have the same slope ( $\partial f/\partial v$ ) and this fact is consistent with a half spherical

2001/04/14, (Left) S/C-1 07:23:18 UT, (Right) S/C-3 07:23:22 UT

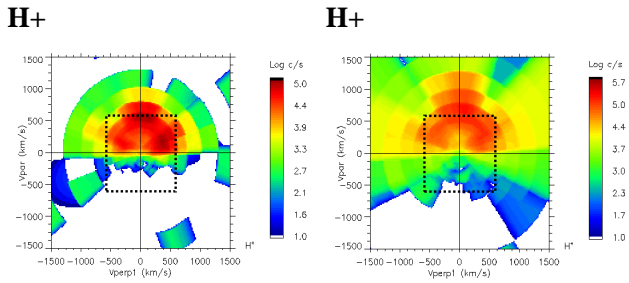


**Fig. 6.** H<sup>+</sup> ion velocity distributions in counts per second (c/s) observed by the Cluster S/C-1 at 07:23:18 UT (left) and the Cluster S/C-3 at 07:23:22 UT (right) on 14 April 2001. There was a 4-s time interval between two spacecraft, but as shown in the velocity distributions, the Cluster S/C-1 was presumed not to be in the dayside cusp due to little down-going population compared to the right one.

shell configuration seen in the H<sup>+</sup> velocity distribution. The broader higher velocity part in  $f(V_{\text{perp}})_{\text{H}^+}$  might come from transverse heating. On the whole, the characteristics of distribution functions are common for two different spacecraft observations.

### 2.3 Velocity distributions in the dayside cusp

Figure 5 shows another configuration seen in O<sup>+</sup> ion velocity distributions both observed in the Southern Hemisphere on 13 February 2001 and 14 April 2001, and the observation conditions were as mentioned in the previous section. In these cases, the spacecraft were in the dayside cusp according to the geomagnetic field components (middle and bottom panel in Fig. 1), and the observation times are shown by a vertical dashed line with number 1), respectively.  $V_{\text{par}} > 0$  corresponds to the upward direction along the geomagnetic field. As to the adjacent observation in the case of 14 April 2001, H<sup>+</sup> ion velocity distribution, whose figure is on the left in Fig. 6, (S/C-1) shows little down-going population apparently compared to the right one (S/C-3). Hence the spacecraft S/C-1 was not presumed to be in the cusp yet at that time. Actually the configuration seen in the O<sup>+</sup> ion velocity distribution at 07:23:18 UT, preceding the spacecraft S/C-3 by 4 s, was neither similar to the configurations in Fig. 5 nor structured (not shown). Configurations seen in both O<sup>+</sup> velocity distributions in Fig. 5 form shell-like structures. Furthermore, in detail according to the cross sections in the  $V_{\text{perp}}$  plane, this configuration is more like a “dome” shape rather than a shell. However, the maximum energy of O<sup>+</sup> ions was probably above the energy  $\sim 40$  keV, equivalent to  $V = 690$  km/s with a detectable upper limit by the instrument, in fact leaving uncertainty about a configuration. In Fig. 7 the distribution functions in the case of 13 February 2001 at 19:48:33 UT observed by the Cluster S/C-1, whose corresponding velocity distributions in the lower panel of Fig. 5, are shown. The construction of this figure is the same as that

of Fig. 4, except  $f(V_{\text{par}} > 0)$  corresponds to an upward-going population along the geomagnetic field. The  $f(V_{\text{par}} > 0)$  and  $f(V_{\text{perp}})$  consist of two distributions clearly, and the higher mean velocity is about  $500 (\pm 200)$  km/s. In spite of an energy (velocity) resolution, which is not good the distribution functions indicate also the emergence of a shell-like (or a dome-shaped) configuration in the O<sup>+</sup> ion velocity distribution.

### 2.4 Overview of evolution of velocity distributions

Figure 8 shows the summary of the evolution of the O<sup>+</sup> ion velocity distribution. The observation times are shown in the middle and bottom panels of Fig. 1, with vertical dashed lines marked by numbers 1) and 2), respectively. The left panels correspond to velocity distributions in the dayside cusp, and a “dome” configuration was seen in the O<sup>+</sup> ion velocity distribution. The right panels correspond to velocity distributions not in the dayside cusp, but perhaps in the mantle region and a shell-like or a pre-shell configuration was seen in the O<sup>+</sup> ion velocity distribution. Regarding a shell-like or a pre-shell configuration in the O<sup>+</sup> ion velocity distribution, in both cases shown in Fig. 8 a cold population (narrow-banded energy) is seen along the geomagnetic field line, but the mean velocity of this cold population is different. The case of 14 April 2001, 08:19:11 UT, might be the earlier stage of evolution of a shell configuration. On the other hand, as to the H<sup>+</sup> ion velocity distribution, a “conic” form is seen in the case of 14 April 2001, 08:19:11 UT, and the region where the spacecraft has crossed is supposed to be the mantle region due to an almost non-existent down-going population. The cases of 13 February 2001, 20:16:19 UT, and 14 April 2001, 07:23:22 UT, were presumed to be observed almost at the edge of the cusp for the former and at the boundary nearby the cusp for the latter, according to the geomagnetic field components and the down-going H<sup>+</sup> population in the velocity distribution.

## 3 Discussion and summary

In this report shell-like configurations seen in the O<sup>+</sup> ion velocity distributions observed in different regions (mantle or dayside cusp) were presented and also compared to the H<sup>+</sup> ion velocity distribution, which is the major ion species in the both observation regions. In the case of 12 April 2001, the O<sup>+</sup> ion number density was nearly constant at  $0.1 \text{ cm}^{-3}$ , whereas that of the H<sup>+</sup> ions was around  $1.0 \text{ cm}^{-3}$ , with one order of magnitude fluctuation (not shown); thus, H<sup>+</sup> was a major ion species. With respect to a “shell-like” distribution, solar wind H<sup>+</sup>/O<sup>6+</sup> distribution functions in the magnetosheath are compared mutually in Fig. 2b by Fuselier et al. (1988) and discussed there. As seen in both upper/lower panels labeled (1) of Fig. 4,  $V_{\text{par}} - V_{\text{perp}}$  distributions have a shoulder at  $|V_{\text{par(perp)}}| \gtrsim 300$  km/s. This kind of shoulder seen in Fig. 2b presented by Fuselier et al. (1988) (clearly seen in the perpendicular distributions of H<sup>+</sup> and He<sup>2+</sup>) was

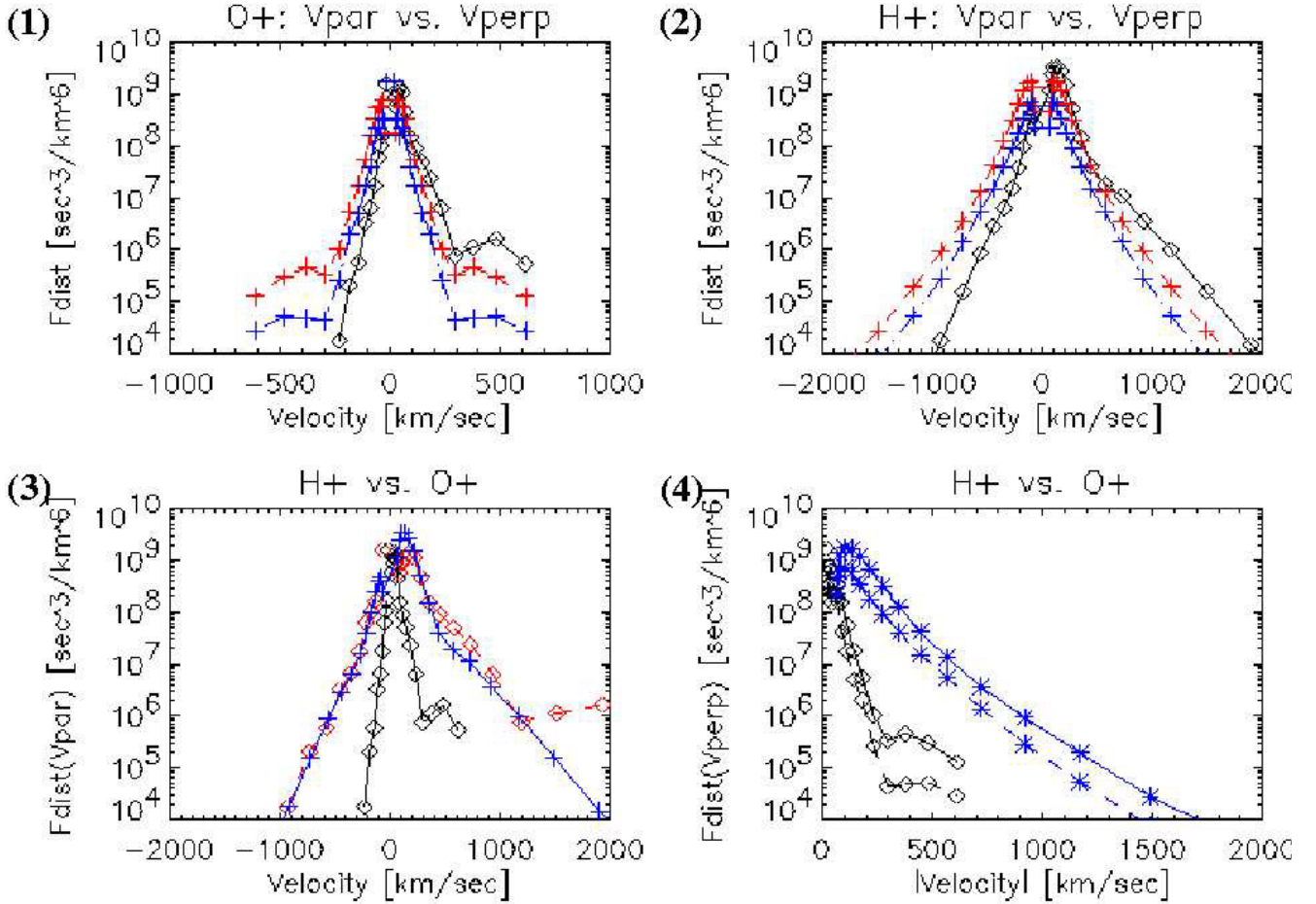


**Fig. 7.** The distribution functions at 19:48:33 UT on 13 February 2001, observed by the Cluster S/C-1. The construction of the figure is the same as that of Figure 4. These distribution functions are considered to be observed in the dayside cusp.

mentioned as attributed to reflected gyrating ions, and Fuselier et al. (1988) also mentioned that the reflected gyrating H<sup>+</sup> ions are a major free energy source for turbulence that may scatter O<sup>+</sup>. In Fig. 4, on the other hand, shoulders can be seen slightly in H<sup>+</sup> distribution functions. Regarding reflected gyrating ions or the “shoulder” in the distribution function, it is much clearer in Fig. 7. There is a much obvious shoulder in the upward-going H<sup>+</sup> population than in the downward-going one, and in the upward-going O<sup>+</sup> population there are two distributions that are well separated.

Fuselier et al. (1988) also suggested the generalised Peterson model (Peterson et al., 1993a) to explain the formation of the He<sup>2+</sup> and O<sup>6+</sup> shell-like velocity distributions in the H<sup>+</sup> rest frame of the solar wind in the Earth’s magnetosheath. The initial distribution of the minor ion species (He<sup>2+</sup> and O<sup>6+</sup>) forms a gyrotropic ring-beam distribution centred at velocity  $V_{0\parallel}$  along the magnetic field, with radius  $V_{0\perp}$  across the magnetic field in the general case when the orientation of the magnetosheath field,  $B$ , and decelerated solar wind velocity,  $V$ , are not aligned. Scattering of this ring-beam into a shell is driven by the magnetic turbulence in the magnetosheath; in particular Fuselier et al. (1988) suggested that

turbulence generated self-consistently by the minor ions may also scatter the initial ring-beam distributions into a shell, and mentioned three critical parameters on which the formation of shell-like distributions depends: the most unstable electromagnetic mode, its growth rate, and the level of pre-existing turbulence in the magnetosheath. The most unstable electromagnetic mode and its growth rate depend on  $V_{0\parallel}$  and  $V_{0\perp}$  of the initial ring-beam distribution, according to the study of lithium ion ring-beam instabilities (Winske et al., 1985).

A shell-like velocity distribution has also been observed previously in newborn cometary ions and Gary et al. (1988) investigated the possibility that it is large-amplitude and lower-frequency magnetic field fluctuations that cause a shell-like ion velocity distribution. According to the work by Gary et al. (1988), an empirical relation for the peak energy density of the magnetic field fluctuations was derived from one-dimensional computer simulations of the R-mode ion cyclotron resonant instability:

$$\frac{|\Delta B|^2}{B^2} \simeq 10 \left( \frac{m_b}{m_c} \right)^2 \left( \frac{v_b}{V_A} \right)^2 \Omega_p \tau_b, \quad (1)$$

where  $m_b$  is the mass of the beam ions (in our case, O<sup>+</sup>

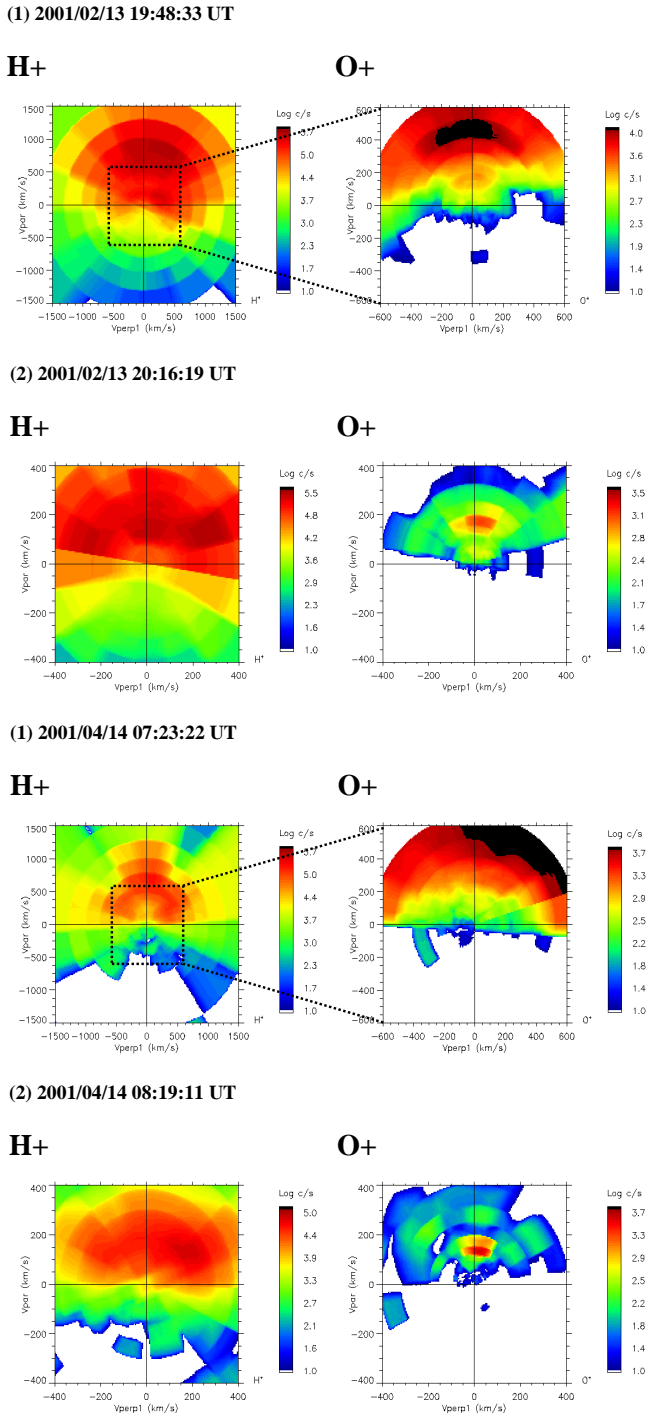


**Fig. 8.** Evolution of O<sup>+</sup> ion velocity distribution. The figures marked by (1) and different date are presumed to be velocity distributions in the dayside cusp. The figures marked by (2) on the right hand are velocity distributions in the mantle region. O<sup>+</sup> ion velocity distributions are different in the dayside cusp or in the mantle region: dome shape rather than shell configuration in the cusp, while pre-shell configuration in the mantle.

ions),  $m_c$  that of the background ions (in our case, H<sup>+</sup> ions),  $v_b$  the relative drift velocity between beam ions and background ions,  $\Omega_p$  the gyrofrequency of protons, and  $\tau_b$  the beam injection time scale. As mentioned previously, the number densities of H<sup>+</sup> and O<sup>+</sup> in the case of 12 April 2001 are  $1.0\sim 10.0\text{ cm}^{-3}$  and  $0.1\text{ cm}^{-3}$ , respectively; thus, O<sup>+</sup> ions can be regarded as beam and H<sup>+</sup> ions can be regarded as background. The fluctuation of the geomagnetic field was roughly estimated by means of a 4-s resolution data of the FluxGate Magnetometer (FGM) instrument on board the Cluster S/C-4, and  $\Delta B/B$  increased from  $10^{-4}$  to  $10^{-2}$  during the observation period on 12 April 2001 (not shown), but the least required energy density for pitch-angle scattering was reported to be  $(\Delta B/B)^2 \gtrsim 10^{-2}$ . Therefore, the level of magnetic turbulence in the mantle or the dayside cusp region, which is supposed to cause scattering ions into shell-like distribution, should be investigated. Further investigation is required with higher resolution of the geomagnetic field data. On the basis of two previous studies mentioned above, our future work concerning shell-like distribution functions of ions will be to look at the interaction between electromagnetic waves and particles where two ion species coexist and the characteristics of geomagnetic field fluctuation (or turbulence) in the dayside magnetosphere. Furthermore, ion energisation mechanisms in terms of wave-particle interactions should also be investigated, i.e. in the BBELF or LH wave modes. The question of whether a shell-like ion velocity distribution is a common phenomena or not should also be answered; therefore, a statistical study on occurrence, location, and other factors/conditions for shell-like velocity distributions will also be done.

*Acknowledgements.* The CIS data and analysis tool are provided by CNES, Toulouse in France. The ACE/MAG data in level 2 are distributed by the ACE Science Centre at Caltech, California, and  $K_p$  index are distributed by the World Data Centre of Magnetism at Danish Meteorological Institute, Solar-Terrestrial Physics Division, Copenhagen. The FGM data was distributed by the Cluster Science Data Centre (CSDC)/the Scandinavian Data Centre (SDC) at the Royal Institute of Technology (KTH), Stockholm.

Topical Editor T. Pulkkinen thanks J. Chen and T. E. Moore for their help in evaluating this paper.

## References

- Bouhram, M., Dubouloz, N., and Malingre, M., et al.: Ion outflow and associated perpendicular heating in the cusp observed by Interball Auroral Probe and FAST Auroral Snapshot, *J. Geophys. Res.*, 107, SMP4(1–13), 2002.
- Brown, D. G., Wilson, G. R., Horwitz, J. H., and Gallagher, D. L.: “Self-consistent” production of ion conics on return current region auroral field lines: A time-dependent, semikinetic model, *Geophys. Res. Lett.*, 18, 1841, 1991.
- Chen, J., Fritz, T. A., Sheldon, R. B., et al.: A new temporarily confined population in the polar cap during the 27 August 1996 geomagnetic field distortion period, *Geophys. Res. Lett.*, 24, 1447, 1997.
- Chen, J. and Fritz, T.: Energetic oxygen ions of ionospheric origin observed in the cusp, *Geophys. Res. Lett.*, 28, 1459, 2001.

- Fritz, T. A., Chen, J., and Siscoe, G. L.: Energetic ions, large diamagnetic cavities, and Chapman-Ferraro cusp, *J. Geophys. Res.*, 108, SMP17(1–9), 2003.
- Fuselier, S. A., Shelley, E. G., and Klumpar, D. M.: AMPTE/CCE Observations of Shell-like He<sup>2+</sup> and O<sup>6+</sup> Distributions in the Magnetosheath, *J. Geophys. Res.*, 15, 1333–1336, 1988.
- Gary, S. P., Madland, C. D., Omidi, O., and Winske, D.: Computer Simulations of two-pickup-ion instabilities in a cometary environment, *J. Geophys. Res.*, 93, 9584, 1988.
- Huebner, W. F.: *Physics and Chemistry of Comets*, Springer-Verlag Berlin Heidelberg, 1990.
- Lavraud, B., Dunlop, M. W., Phan, T. D., et al.: Cluster observations of the exterior cusp and its surrounding boundaries under northward IMF, *Geophys. Res. Lett.*, 29, 1995, doi:10.1029/2002GL015464, 2002.
- Lund, E. J., Möbius, E., Carlson, C. W., et al.: Transverse ion acceleration mechanisms in the aurora at solar minimum: occurrence distributions, *J. Atmos. Terr. Phys.*, 62, 467, 2000.
- Moore, T. E., Waite Jr., J. H., Lockwood, M., and Chappell, C. R.: Observations of coherent transverse ion acceleration, in: *Ion Acceleration in the Magnetosphere and Ionosphere*, Geophys. Monogr. Ser., edited by Chang, T. and AGU, Washington D.C., vol.38, 50, 1986.
- Mukai, T., Miyake, W., Terasawa, T., Kitayama, M., and Hirao, K.: Plasma observation by Suisei of solar-wind interaction with comet Halley, *Nature*, 321, 299, 1986.
- Neugebauer, M., Lazarus, A. J., Alwegg, K., Balsiger, H., et al.: The pick-up of cometary protons by the solar wind, *Astron. Astrophys.*, 187, 21, 1987.
- Nordqvist, P., André, M., and Tyrland, M.: A statistical study of ion energization mechanisms in the auroral region, *J. Geophys. Res.*, 103, 23 459, 1998.
- Peterson, W. K., Shelley, E. G., Sharp, R. D., et al.: H<sup>+</sup> and He<sup>++</sup> in the dawnside magnetosheath, *Geophys. Res. Lett.*, 6, 667, 1979.
- Peterson, W. K., Yau, A. W., and Whalen, B. A: Simultaneous observations of H<sup>+</sup> and O<sup>+</sup> ions at two altitudes by the Akebono and Dynamics Explorer 1 satellites, *J. Geophys. Res.*, 98, 11 177, 1993a.
- Peterson, W. K., Abe, T., André, M., et al.: Observations of a transverse magnetic field perturbation at two altitudes on the equatorward edge of the magnetospheric cusp, *J. Geophys. Res.*, 98, 21 463, 1993b.
- Roth, I. and Hudson, M. K.: Lower Hybrid heating of ionospheric ions due to ion ring distributions in the cusp, *J. Geophys. Res.*, 90, 4191, 1985.
- Winske, D., Wu, C. S., Li, Y. Y., et al.: Coupling of newborn ions to the solar wind by electromagnetic instabilities and their interaction with the bow shock, *J. Geophys. Res.*, 90, 2713, 1985.
- Yau, A. W. and André, M.: Sources of ion outflow in the high latitude ionosphere, *Space Sci. Rev.*, 80, 1–25, 1997.